New IR-UV gas sensor to energy and transport sector

Fateev, Alexander; Clausen, Sønnik

Publication date:
2010

Document Version
Publisher's PDF, also known as Version of record

New IR-UV gas sensor to energy and transport sector

Risø-R-Report

Alexander Fateev and Sønnik Clausen
PLF Programme
Risø-R-1758(EN)
December 2010

Risø DTU
National Laboratory for Sustainable Energy

Author: Alexander Fateev and Sønnik Clausen
Title: New IR-UV gas sensor to energy and transport sector
Division: PLF programme

Risø-R-1758(EN)
December 2010

Abstract (max. 2000 char.):

In situ simultaneous measurements of gas temperature and gas composition are of great interest in combustion research and give useful information about conditions, chemical reactions and gas mixing in many industrial processes. An optically based technique is beneficial because it is non-intrusive, accurate, fast and can be performed *in situ* for various extremely hard conditions. In humid and hot gas flows UV technique is more sensitive than FTIR one for fast gas concentration measurements of NO and SO_2 and gives a great opportunity for simultaneous measurements of O_2 concentration. Analysis of the fine structure of the UV absorption bands of, for example, NO, SO_2 or O_2 allows also to determine a value of the gas temperature. Absorption cross sections of CO_2, H_2O and SO_2 at elevated temperatures are reported. Design of a new developed 9-m long water-cooled fiber-optic probe with removable optical head suitable for fast IR/UV local gas absorption/emission measurements is described. The probe performance was successfully tested in several trial measurements on full scale multi-fuel fired boiler. A concept of fast time/spectral-resolved measurements has been used in measurements on a large ship engine.

ISSN 0106-2840
ISBN 978-87-550-3869-1

Contract no.:
Energinet.dk Project No 2007-7319

Group's own reg. no.:
1750181-01

Sponsorship:

Cover :
UV-head mounted onto 9-m water-cooled probe inserted at a superheater level at Avedøre Power Station (Block 2), Copenhagen

Pages: 33
Tables:2
References: 22

Information Service Department
Risø National Laboratory for Sustainable Energy
Technical University of Denmark
P.O.Box 49
DK-4000 Roskilde
Denmark
Telephone +45 46774005
bibl@risoe.dtu.dk
Fax +45 46774013
www.risoe.dtu.dk

Contents

Preface

The report describes the work carried out in the Energinet.dk project No. 2007-7319. Multi component gas analyzer system combining IR/UV measurement techniques are described. A possibility of integration IR and UV spectroscopy for sensitive fiber optic measurements of NO, SO_2 and at elevated temperatures O_2 over a short optical path is shown. Developed concept can be used on various industrial environments, e.g. burners and engines.

1 Introduction

In situ simultaneous measurements of gas temperature and gas composition are of great interest in combustion research and give useful information about conditions, chemical reactions and gas mixing in many industrial processes. Usually gas measurements have to be done in a very aggressive and unstable in time hot gas environment which is realized, for example, in boilers and engines. Experimentally measured values of temperature and gas composition in various positions in the boilers can be used for advanced combustion diagnostics and for validation and improvement of CFD codes those now are recognized as an obligatory tool in boiler design and optimization.

An optically based technique is beneficial because it is non-intrusive, accurate, fast and can be performed *in situ* for various extremely hard conditions. Fast Fourier Transform Infrared (FTIR) spectroscopy for *in situ* optical diagnostics of hot gases has extensively been developed for many years in Optical Diagnostics Group at Risø DTU and has successfully been used in practice on various industrial sites in Denmark and Europe [1]. In humid and hot gas flows ultraviolet (UV) technique is more sensitive than FTIR one for fast gas concentration measurements of NO and SO_2 and gives a great opportunity for simultaneous measurements of O_2 concentration. Analysis of the fine structure of the UV absorption bands of, for example, NO, SO_2 or O_2 allows also to determine a value of the gas temperature.

Advanced laser-based diagnostic methods developed in the past tenths years are successfully used for lab, small and for a less extend medium scale combustion systems [e.g. 2, 3]. However they are difficult to apply on the full scale. Industrial combustion control by conventional emission/absorption spectroscopy is very common and mainly used for a qualitative (UV-VIS) and quantitative (IR) line of sight cross stack combustion monitoring [e.g. 4, 5].

In the report design of a new developed 9-m long water-cooled fiber-optic probe with removable optical head suitable for fast IR/UV local gas absorption/emission measurements is described. The probe performance was successfully tested in several trial measurements on full scale multi-fuel fired boiler. Measurements have been performed at various fuel loads and fuel composition and up to 8 m inside of the hot gas flow close to the superheater region of the multi-fuel boiler at Avedøre power station (Unit 2: AVV2) located south of Copenhagen [6]. In Ch. 2 measurements of absorption cross sections of CO_2, H_2O and SO_2 are reported. Experimental layout for probe and optical set-up is described in Ch's. 3.1 and 3.2. Examples of fast UV absorption measurements at various combustion conditions are presented in Ch 3.3. Fast absorption measurements in natural gas combustion are discussed in details and compared with traditional gas extraction measurements and data available from the control and data system of the boiler. A method for data analysis of the UV spectra allowing one to get both gas temperature and gas composition is also described. A concept of fast time/spectral-resolved measurements described in the Ch. 3 has been used in measurements on a large ship engine at MAN Diesel facilities in Copenhagen described in Ch. 4.

2 UV-spectroscopy set up on high temperature gas cell

In order to make an analysis of complex UV absorption spectra, tools for calculation of absorption spectra species of interest at certain temperatures have to be developed. In case of diatomic molecules like O_2 and NO such calculations can be done in order to match to reference absorption spectra even at high temperatures. A reference absorption spectrum is defined as an absorption spectrum of specie of interest at certain concentration, temperature, optical absorption path length and spectral resolution of the instrument. In case of polyatomic molecules, e.g. CO_2 or SO_2 there is a leak of high temperature absorption cross section databases because 1) considerable complications in *ab initio* spectral calculations at high temperatures and 2) availability of UV high temperature absorption cross sections accurately measured at various temperatures. In the next chapters measurements of CO_2, H_2O and SO_2 UV absorption cross sections in Risø DTU high temperature flow gas cell (HGC) are reported.

2.1 Atmospheric pressure high temperature flow gas cell

Measurements have been performed on Risø DTU atmospheric-pressure high-temperature flow gas cell (HGC) [7]. The gas cell was designed as a flow gas cell with a so-called laminar window, nozzle seal cell principle, where care was taken to obtain a similar uniform gas temperature profile and well defined path length as for the other two gas cells with hot windows in our laboratory.

The HGC consists of three different parts: a high-temperature sample cell with a length of 53.3 cm and two “buffer” cold gas parts on the left- and the right-hand sides of the hot sample cell. The buffer parts are filled by a UV/IR-transparent (purge) gas (e.g. N2), whereas the central sample cell can be filled by the gas under investigation (e.g. N_2+CO_2). The aperture of the sample cell is kept small (i.e. a diameter of 1.5 cm) in order to reduce heat transfer by radiation from the sample cell and to reduce the risk of collapse of well-defined flows in the laminar windows. The laminar windows also function as a radiation shield. Similarly, apertures placed at the end parts between the laminar windows and the cold windows reduce the heat losses by radiation and convection by breaking down the vortices created by the thermal gradient in the buffer sections. High-quality pure ceramics were used in order to minimize hetero-phase reactions and to avoid contact of the sample gas with any hot metal parts. A uniform temperature profile is obtained by heating the gas cell with a dedicated three-zone furnace in order to compensate for the heat loss at the ends of the gas cell. The sample gas is preheated. Flows of the gases in the sample cell and in the buffer parts are kept at about the same flow rates. The outer windows placed on the ends of the buffer parts are replaceable. In all experiments, KBr-windows have been used. The gas flow through the HGC maintains a highly uniform and stable temperature in the range 23°C to 1600°C and pressure is around 1 bar. Temperature uniformity along the axis of the high-temperature central part of the HGC were verified by thermocouple measurements at three different points inside the HGC The temperature uniformity over 0.45 m in the central part of HGC was found to be better than ±1ºC, or on average ±0.5°C. Further

details of the HGC, its performance and comparison with our others high temperature flow gas cells will be presented and discussed in another paper [8].

2.2 CO_2, H_2O and SO_2 UV absorption cross sections at high temperatures

UV absorption spectra of polyatomic molecules are complicated and consist from various absorption bands overlapping with each other. The spectral resolution of a spectrometer in UV is normally not enough to resolve a fine structure in the absorption spectra. Therefore in the most cases absorption cross sections, reported in the literature are instrument dependent (so-called apparent cross sections, $\sigma^{app}(\nu,T)$). UV high temperatures absorption spectra of H_2O and CO_2 show continue-like structure without any characteristic features. In opposite, an UV absorption spectrum of SO_2 shows two maxima with some temperature-pressure dependent "saw"-like structure [9].

In order to have high-quality $\sigma^{app}(\nu,T)$ reference data for H_2O, CO_2 and SO_2 several high-resolution absorption measurements on HGC were performed. High-resolution UV-absorption measurements ($\Delta\lambda$=0.046 nm) were done with a 0.5 m UV-optimized spectrometer equipped a CCD-camera. A highly-stable deuterium lamp (LOT) with a UV-condenser was utilized as a parallel-beam light source in the range 190-400 nm. UV light beam, after passing through the HGC, was focused by means of a SUPRASIL lens into the head of a 1 m long solarization-resistant fused-silica optical fiber (LOT) coupled to the entrance slit of the UV spectrometer.

Apparent absorption cross sections of H_2O, CO_2 and SO_2 in the range 800-1500^{o}C with step 100^{o}C have been measured. In Fig. 2.1 and 2.2 examples of high-resolution absorption cross sections of CO_2 (T=1500^{o}C) and H_2O (T=1300^{o}C) are shown by the red lines. Because apparent absorption cross sections have continuum-like smoothed behavior they can be described with a functional form [10]

$$\ln\sigma(\lambda,T)^{app} = a(T) + b(T)\lambda\,, \qquad (1)$$

where

$a(T) = c_1 + c_2T + c_3T^{-1}$ and $b(T) = d_1 + d_2T + d_3T^{-1}$.

In the work [10] parameters c_i and d_i for H_2O and CO_2 absorption were calculated for 190-210 nm and 200-320 nm spectral ranges from the UV absorption spectra in shock-heated gas mixtures of H_2O and CO_2 with Ar at temperatures varied between 630^{o}C and 2777^{o}C. Calculated $\sigma(\lambda,T)^{app}$ for CO_2 and H_2O with use of the Eq. 1 and parameters c_i and d_i from [10] are shown in the Fig. 2.1 and 2.2 by blue lines. There is a good agreement between our $\sigma(\lambda,T)^{app}$ measurements in HGC and calculated "parameterized" ones. In this work (see below) $\sigma(\lambda,T)^{app}$ calculated from the Eq. 1 were used in the analysis of the experimental data.

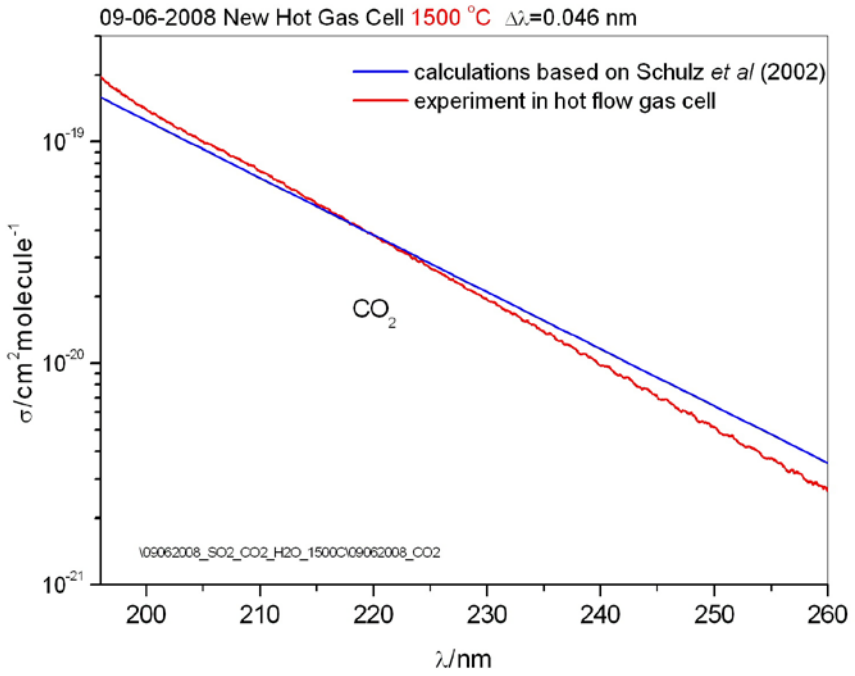

Figure 2.1: Absorption cross section of CO_2 measured in HGC at T=1500°C (red) and calculated one based on Schulz *et al* [10] (blue)

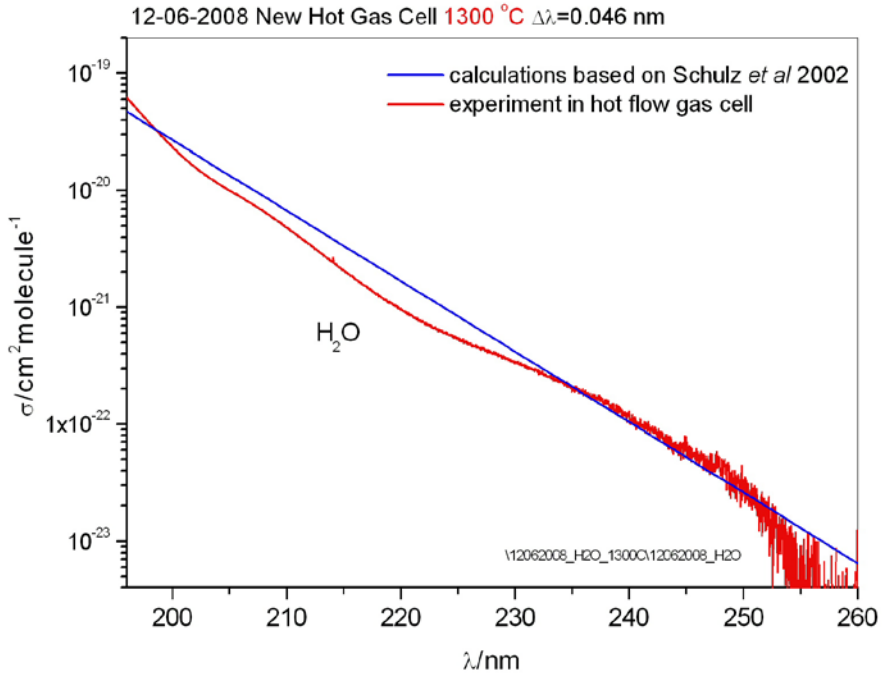

Figure 2.2: Absorption cross section of H_2O measured in HGC at T=1300°C (red) and calculated one based on Schulz *et al* [10] (blue).

Absorption cross sections of SO_2 were extensively measured at temperatures below 20°C. Excellent compilation of SO_2 absorption cross sections in VUV-UV ranges is presented in MPI-Mainz-UV-VIS-Spectral Atlas of Gaseous Molecules [9]. In Fig. 2.3 SO_2 absorption cross sections taken from the work [11] at 20°C and $\Delta\lambda$=0.1 nm (blue line) are shown in comparison with our measurements in 50 cm length gas cell used in gas extraction experiments at 150°C and $\Delta\lambda$=0.032 nm (red line). One can see that at 150°C the fine structure of the SO_2 absorption bands becomes broader compare to 20°C due to the temperature but in general the shape of $\sigma(\lambda,T)^{app}$ is still preserved.

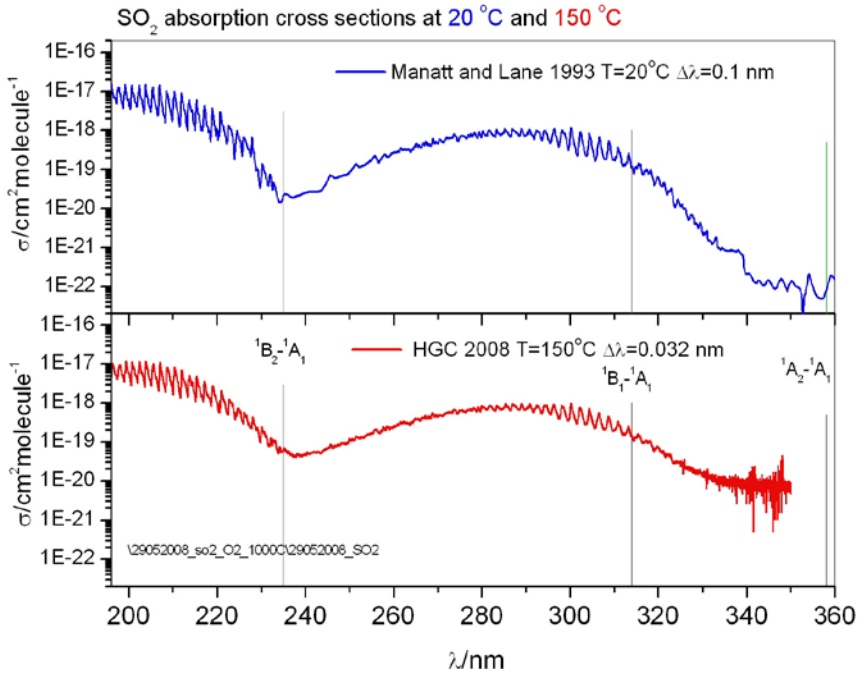

Figure 2.3: Absorption cross section of SO_2 at T=150°C measured in HGC ($\Delta\lambda$=0.032 nm, red). Absorption cross section from the work Manatt and Lane [11] at 20°C is shown for comparison ($\Delta\lambda$=0.1 nm, blue). Vertical lines show positions of origins for three SO_2 absorption bands.

The SO_2 UV absorption is complicated. The spectrum consists from three different bands with blue progressions and their origins shown in Fig. 2.3 by vertical lines, namely $\tilde{A}\,^1A_2 \leftarrow \tilde{X}\,^1A_1$ (358 nm), $\tilde{B}\,^1B_1 \leftarrow \tilde{X}\,^1A_1$ (314 nm) and $\tilde{C}\,^1B_2 \leftarrow \tilde{X}\,^1A_1$ (235 nm). The smooth progression of sharp lines $\tilde{A} \leftarrow \tilde{X}$ breaks down near 299 nm with followed overlap with more complex structure of $\tilde{B} \leftarrow \tilde{X}$ underlying $\tilde{A} \leftarrow \tilde{X}$ band system in 290-314 nm. At temperatures below 20°C the band $\tilde{B} \leftarrow \tilde{X}$ is disappearing down to 235 nm. More detailed discussion about SO_2 spectroscopy is outside of the scope of this report and can be found elsewhere, e.g. [12].

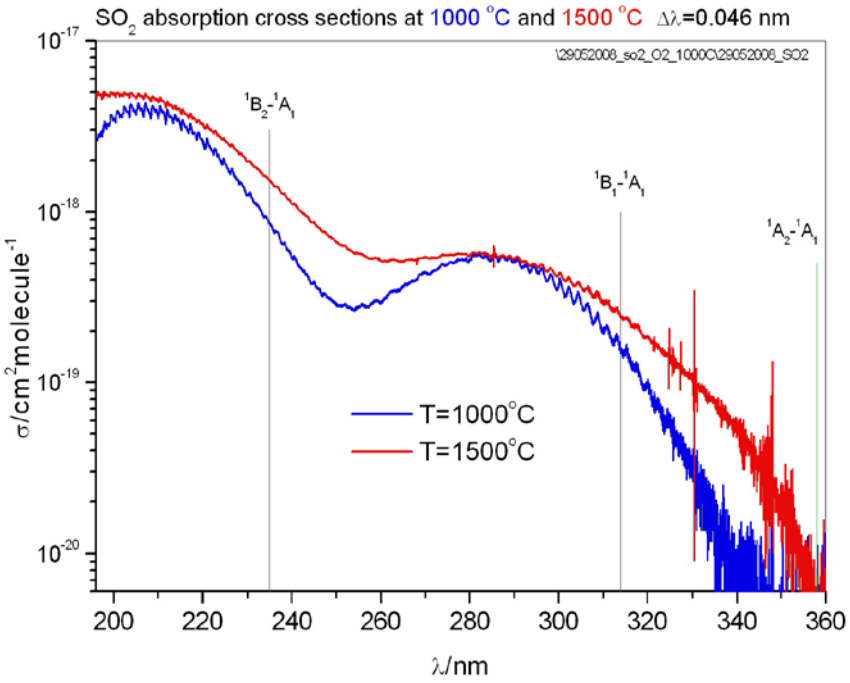

Figure 2.4: Absorption cross sections of SO_2 measured in HGC at T=1000°C (blue) and 1500°C (red). Vertical lines show positions of the origins for three SO_2 absorption bands.

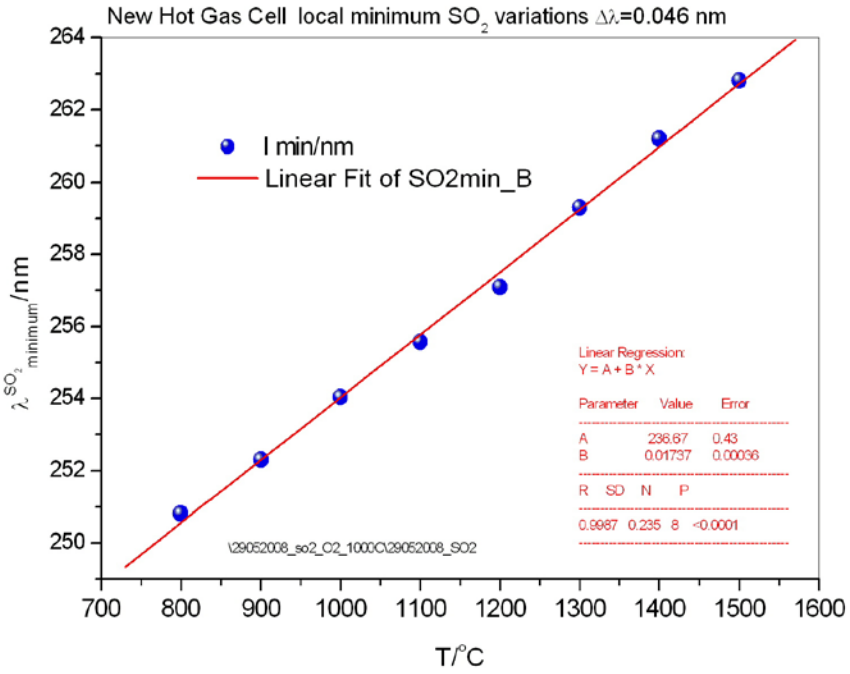

Figure 2.5: Position of a local SO_2 absorption minimum between $^1B_2$-$^1A_1$ and $^1B_1$-$^1A_1$ bands as a function of the gas temperature in HGC from 800 to 1500°C (blue balls) and it fit by a line function (red line).

Heating of the SO_2 to a temperature more than 150^{o}C leads to several changes in the UV absorption spectrum. In Fig. 2.4 two high-resolution SO_2 absorption cross section spectra at 1000^{o}C (blue) and 1500^{o}C (red line) measured in HGC are shown. The absorption spectra become smooth and broader due to redistribution in the ground state vibrational levels population with still remaining structured features in $\tilde{C} \leftarrow \tilde{X}$ and $\tilde{A} \leftarrow \tilde{X}$ bands, Fig. 2.4.

The other observation that might be seen from the Fig. 2.4 is a red-shift of the minimum between two $\tilde{C} \leftarrow \tilde{X}$ and $\tilde{B} \leftarrow \tilde{X}$ bands. Thus at 1000^{o}C this minimum is observed at 254 nm, whereas at 1500^{o}C the minimum is around 263 nm. Our measurements in HGC in the range 800-1500^{o}C show that a position of the SO_2 local minimum is a linear function of the temperature, Fig. 2.5. Therefore SO_2 minimum feature can be used for gas temperature estimation. High-temperature SO_2 absorption measurements in the range between 200 and 400 nm and spectral resolution 0.5 nm were reported in the work [13] at room, 600 and 800^{o}C and absolute pressures between 1 and 6 bar. Another high temperature SO_2 absorption measurements up to 427^{o}C at $\Delta\lambda$=0.23 nm were presented in the work [14]. Higher resolution measurements ($\Delta\lambda$<0.05 nm) at the temperatures up to 1200^{o}C and probably in the range 205-220 nm were mentioned in the reference of the work [15]. To our knowledge SO_2 apparent absorption cross sections reported in the present work are the first high-resolution data available at temperatures up to 1500^{o}C and pressure 1 bar.

3 UV fiber optical set up for *in situ* full-scale measurements

Experimental layout used in *in situ* measurements includes a 9-m long water-cooled probe with removable optical head suitable both for UV and IR absorption measurements and the optical set-up described below.

3.1 Design and test of UV fiber optical head

A removable optical head matching the 9-m long probe suitable for *in situ* UV/IR gas absorption measurements gas has been developed and tested. The optical head was made from AISI 304 stainless steel. In the Fig. 3.1 a transparent view of the optical head without exterior cover is shown. A UV light source is inserted from the front end and kept in the correct position by a spring fixed with the front cap. A fiber adapter/lens module is inserted and fixed from the back side in a ¾ inch thread which is also used for mounting of the optical head onto the 9-m probe through a matching plug. Electrical wires and the purge gas for the UV light source are guided through two channels on the each side of the optical head.

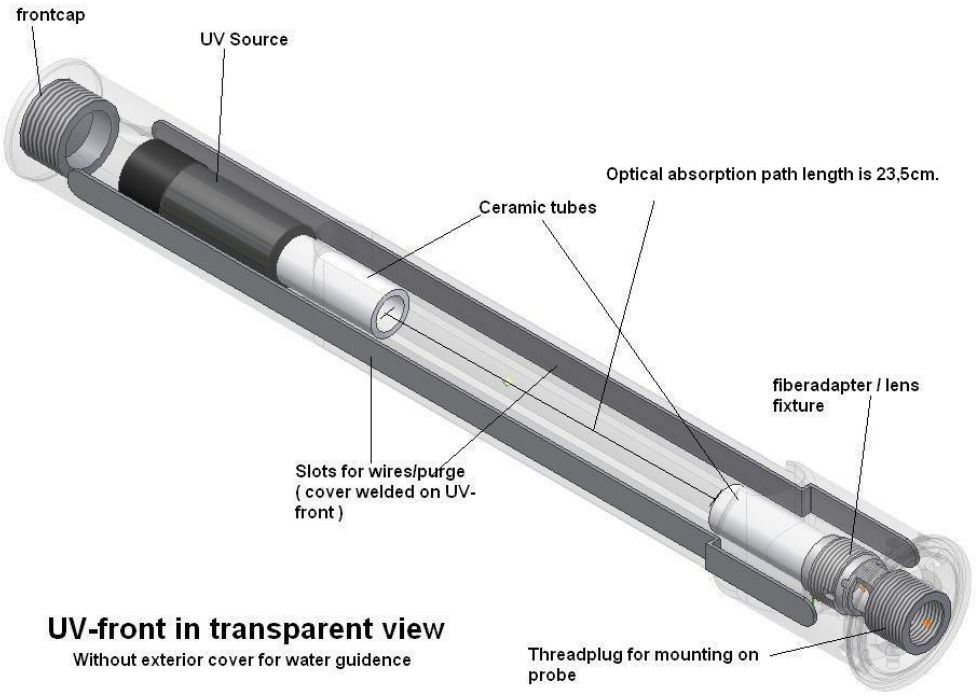

Figure 3.1: UV optical head: transparent view

Cooling water to the optical head is provided from the 9-m probe through a groove in the optical head end that is sealed by two o-rings. Water after passing through the groove is

re-directed to the gap between the optical head main body and exterior cover through ten 5 mm holes. Return water leaves the UV head through 16x1 mm stainless steel tube fixed outside on the 9-m probe.

For protection of the optical components, i.e. the UV light source and lens/fiber module, from the heat radiation and contamination by soot and dust particles two ceramic tubes variable length enclosed in the optical head body are used. The tubes are kept in the place by small spring loaded balls. Small nitrogen purge flow flowing around the source and fiber adapter/lens and next through the ceramic tubes is utilized to keep optics clean. The maximum optical absorption path length (or shortest acceptable ceramic tubes length) between both ends of the ceramic tubes is 23.5 cm. The optical head in operation (with UV light source on) during measurements at AVV2 is shown on the Report's cover.

A stable 20 W deuterium lamp (Cathodeon, model F05) with a plano-convex fused silica lens (LOT) was placed in the optical head and utilized as a parallel-beam light source in the range 190-400 nm. The UV light beam, after passing through a gas column was focused by a plano-convex fused silica lens (ISP optics) placed in fiber adapter/lens module into the entrance of 10-m long premium-grade solarization-resistant quartz fiber with 0.6 mm core diameter (Ocean Optics). The fiber was coupled to a high-resolution spectrometer.

High-resolution UV-absorption measurements were performed with a spectrometer (SpectraPro 2500i, Acton Research) equipped a CCD-camera (PIXIS-100B, Princeton Instruments). The dispersion of the grating (Holographic, 1800 mm^{-1}) was sufficient to cover a spectral range of 28 nm on the CCD. A spectral resolution was $\Delta\lambda$=0.046 nm with an entrance slit width of 40 μm.

3.2 Design and test of 9-m water-cooled probe

The probe was designed for fast *in situ* full scale UV/IR gas absorption measurements in flame or hot flue gas stream based on our previous experience, e.g. [16]. The diameter of the probe, 60 mm, was chosen based on calculations of the heat transfer, mechanical stiffness, cooling water requirements, weight and safe operation demands for the probe operated with insertions up to 8 m into a hot gas flow and temperatures up to 1600^{o}C.

The probe consists of three stainless steel tubes 1-3, Fig. 3.2. The outer tube 3 is made from commercially available the SAF2205 duplex stainless steel having a good strength at high temperature and deep insertions. All other components of the probe are made from the AISI 304 stainless steel. Cooling water is guided between tubes 1 and 2 to the probe front from where it returns back between tubes 2 and 3, Fig. 3.2. Between tubes 1-2 and 2-3 there are spirals twisted around the corresponding inner tube to keep the tubes centered and create vortexes in cooling water flow. The flange 4 is welded together with the tube 1. An o-ring seals between tubes 1 and 2 at the back end.

This design makes possible to insert the probe safely into a high temperature zone of a flame or flue gas without creating any stress on the tubes due to different thermal expansion of the components.

In the flange 4 there is a ¾ inch thread for mounting of the optical head and three holes with M10 mm thread allowing cooling water to reach the optical head. The holes can be

plugged when the optical head is not being in use. An optical fiber is drawn out through the inner part of the tube 1 that is also used as a purge gas flow channel.

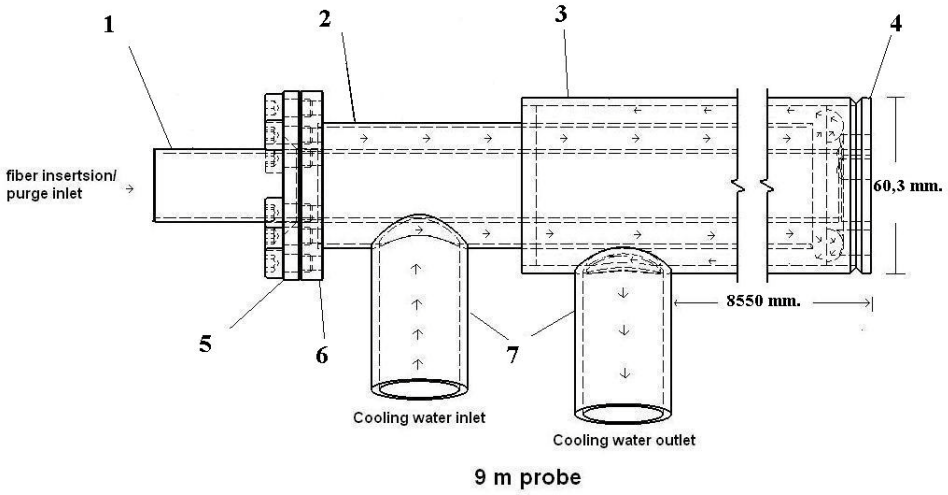

Figure 3.2: The 9-m long probe design

3.3 *In situ* UV absorption measurements at AVV2

The 9-m long probe with the optical head described in the Ch. 3.2 has been used for several *in situ* trial measurements on the AVV2 boiler [6]. All measurements were performed in the superheater region of the boiler and various probe insertion depths. The boiler size at the point of measurements is around 15 x 15 m in horizontal cross section. During all trials the boiler was running in the regime defined by an operator in the control room of the AVV2 and optimized for the best energy production efficiency. Therefore results shown below demonstrate only a potential of the developed technique and data analysis for full scale diagnostics.

3.3.1 Oil, wood and natural gas operation

In the first trial the probe with optical head has successfully been tested to sustain harsh conditions in the superheater region of AVV2 operated with a coal/wood/oil feeding. The maximum insertion depth was 8 m. First acquired UV absorption spectra of SO_2 have been demonstrated a possibility of 30 ms acquisition time measurements.

After several technical improvements in the probe and optical set-up's UV absorption measurements were repeated in the second trial at wood:oil:gas = 0.81:0.15:0.04 feeding. Averaged over time of measurements flue gas composition before $DeNO_x$ unit obtained from AVV2 data-log file was: NO_x=112 ppm, SO_2=362 ppm and O_2=1.7%. Measurements were performed at probe insertion depths of 2 and 4 m inside the boiler. Absorption path length in the optical head was set to 22 cm. Unfortunately during trial the mechanical stability of the fiber coupled to the UV-spectrometer was poor that caused acquisition of $I_0(\lambda)$ and $I(\lambda)$ at different fiber end couplings. Therefore

measurements presented in this chapter are only qualitative ones. The intensities $I_0(\lambda)$ and $I(\lambda)$ were measured when the probe was placed outside and inside of the boiler, respectively. The measurements were performed in 190-240 nm range. Spectra were continuously recorded in one-by-one sequence during around one minute at a selected grating position. Effective acquisition time for each spectrum (or frame) in the sequence was set to 5.4 ms.

A part of the UV absorption data is shown in Fig. 3.3 at grating position 210 nm. The CCD covers spectral range of 28 nm that allows a simultaneous acquisition of several molecular absorption bands or even atomic lines. Two spectra in blue (1) and red (2), Fig. 3.3, were recorded at the 2 m probe insertion and times 0.211 s and 8.301 s after measurements begun, respectively. The blue spectrum (1) has specific oxygen footprints like in the Fig. 4 whereas the red one (2) is mainly shows CO_2 and H_2O absorption with "traces" of O_2 and SO_2. In opposite, the green (3) spectrum in Fig. 3.3 corresponds mainly to high-temperature SO_2 absorption. The spectrum was measured at 4 m probe insertion at 9.137 s after measurements started.

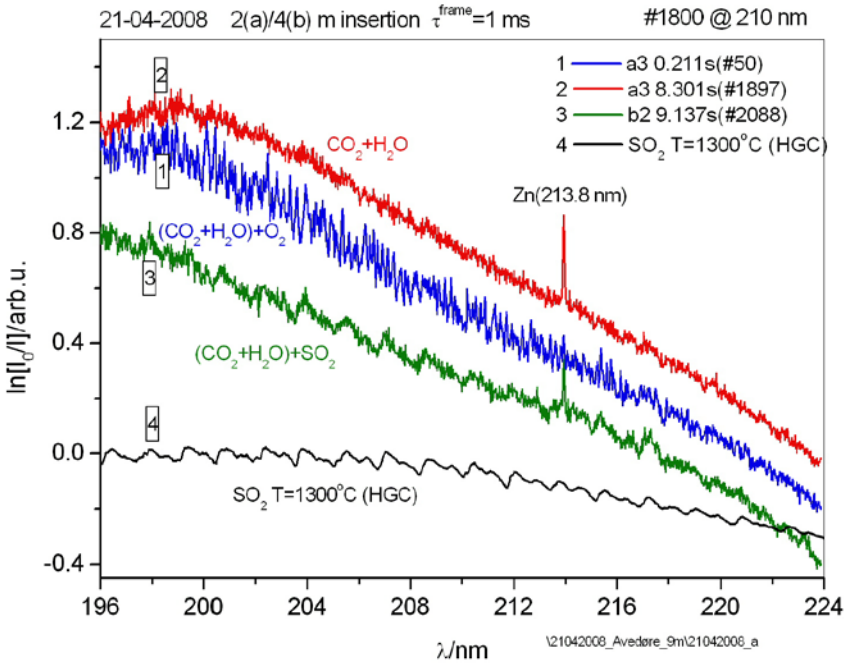

Figure 3.3: 5.4 ms UV absorption measurements at AVV2 with oil, wood and natural gas feeding at various probe insertions: 2 m inside (0.211 s, blue and 8.031 s, red) and 4 m inside (9.137 s, green). An absorption (Y-shifted) spectrum of SO_2 at T=1300°C measured in HGC is also shown for comparison. The grating position is 210 nm.

A typical SO_2(500 ppm) absorption spectrum (shifted in Y direction) at 1300°C measured in our HGC is shown in the Fig. 3.3 (black line, (4)) for a reference. All these absorption patterns (blue, red and green) are observed for several one-by-one measured spectra in the sequence i.e. they exist in time of a few tens of milliseconds. Differences in the absorption spectra can be attributed, for example, by transient gas flow separation

or by combustion development. Three cases shown in Fig. 3.3 illustrate a capability of fast UV absorption measurements for *in situ* optical diagnostic of hot reacting gas flows.

3.3.2 Natural gas operation

As was noted in the previous chapter, due to pure fiber – spectrometer coupling during the second trial measurements obtained data can only be used for qualitative information about hot gas behavior. Prior the third trial two improvements have been done: coupling of the end of the optical fiber to the spectrometer were re-designed and the optical path length in the optical head has been increased to 23.5 cm by shorter ceramic tubes, Fig. 3.1. The third trial measurements were performed during AVV2 natural gas operation at a minimum load. The thermal effect of the boiler was 120 MW_{th}.

Low or dynamic load operations become more important in the present and in particular in the near future due to rapid grow of wind-mills energy market and require better understanding of boiler behavior that is designed for a maximum load operation. Measurements were done at 0.5, 1.5 and 3 m probe insertion depths. The intensities $I_0(\lambda)$ and $I(\lambda)$ were measured when the probe was placed outside and inside of the boiler, respectively.

3.3.3 Fast absorption measurements and data analysis

An example of the absorption signal time variation at wavelengths 200.142 nm and 219.189 nm and 1 m probe insertion is shown in Fig. 3.4 by blue and red lines, respectively. The signals were corrected to soot + fiber absorption in 196-224 nm (below). The first wavelength corresponds to the maximum in the spectra to that contribute 6-2, 9-3 and 12-4 O_2 absorption bands with underlining CO_2 and H_2O continua-like absorption, whereas the second one is on the tale of oxygen absorption where absorption is mainly due to CO_2 and H_2O. One can see a strong time variation in the absorption signal at 200.142 nm and correlation between two signals at 200.142 and 219.189 nm as well. Each point in the Fig. 3.4 corresponds to the frame acquisition time of 5.4 ms. As will be shown below these rapid and strong variations in the absorption signal correspond to simultaneous variations in the gas temperature in gas composition. In the regions marked by solid vertical lines and numbered from 1 to 3 in the Fig. 3.4 the absorption signal is insignificantly changed in time compare to the full absorption range. For the following representative analysis the absorption spectra accumulated in the regions 1, 2 and 3 were averaged that corresponds to an averaging over 17, 18 and 12 frames, respectively.

An example of raw high temperature UV absorption spectra measured in 196-224 nm at 1 m probe insertion and averaged over regions 1, 2 and 3 in the Fig. 3.4 is shown in Fig. 3.5. Spectra consist from O_2, CO_2, H_2O and soot partial absorption patterns and may also contain absorption by nanoparticles like two- to three-ring PAHs [17]. High temperature absorption by molecular gases has been discussed in the previous chapters. Soot has a nearly constant absorption in 196-230 nm range as is shown in [17]. Our UV absorption measurements of fine soot particles taken from delaminated deposit on the UV head and homogeneously distributed in a quartz cuvette for absorption measurements show also nearly constant absorption in 196-360 nm. Therefore in the followed data analysis absorption by soot was assumed as a constant offset in the absorption spectra.

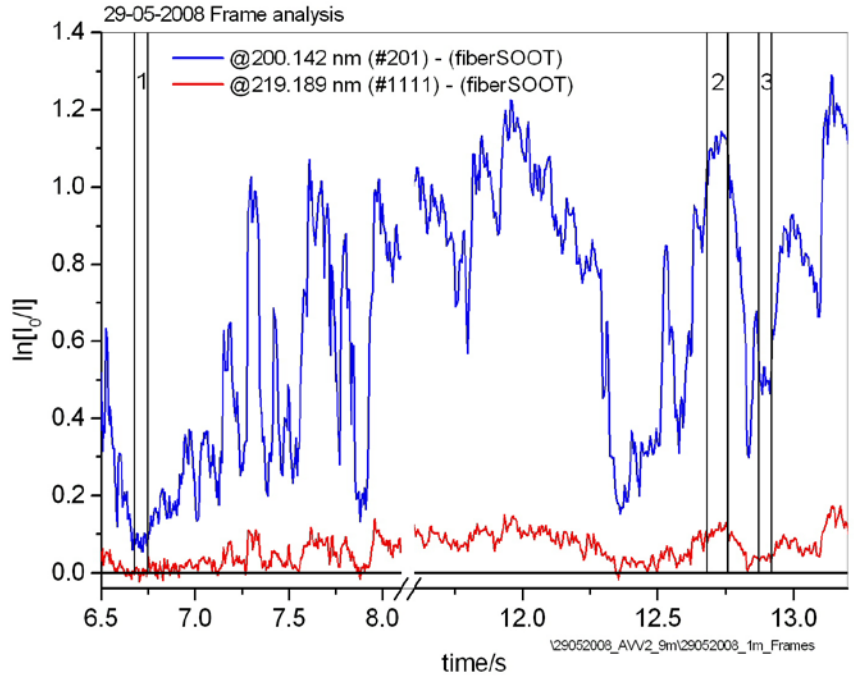

Figure 3.4: A typical time variation of the absorption signal at 200.142 nm (blue) and 219.189 nm (red) with 1 m probe insertion in natural gas minimum load AVV2 operation. In the quasi-stable regions marked by vertical lines and numbered from 1 to 3 absorption spectra were averaged for the followed analysis. Grating position 210 nm.

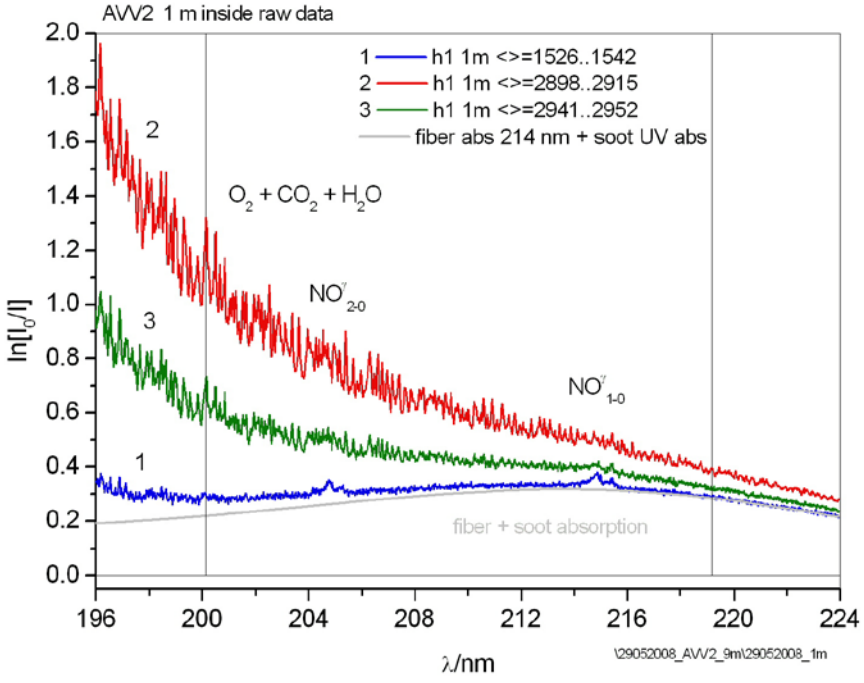

Figure 3.5: Averaged over regions 1, 2 and 3 in Fig. 3.4 raw UV absorption spectra. Vertical lines mark positions 200.142 nm and 219.189 nm of O_2 S-R bands for those time variations of the absorption signal are plotted in Fig. 3.4. Numbers correspond to various regions in Fig. 3.4. Grey line is UV absorption by optical fiber and soot.

Volume fraction of nanoparticles is reduced along the flame height due to coagulation and graphitizing into the burned gas region forming soot particles those volume fraction in opposite is increased [17]. Because our measurements were performed close to the superheater region i.e. far away from the flame top region we have assumed that nanoparticles are appeared in a negligible fraction at least below of the detection limit.

Although in the measurements we used a premium-grade solarization-resistant optical fiber from Ocean Optics, a broad-band absorption by optical fiber with maximum at 214 nm due to solarization effect was observed and verified in a separate set of experiments. Solarization for the fiber used depends on the time on that fiber is exposed under the UV light. For one measurement sequence that lasts for around 45 s changes in the fiber light transmission due to its solarization are minor and an absorption by fiber was assumed to be constant for all spectra in the sequence. Because all O_2, CO_2 and H_2O have weaker absorption at low temperatures their low temperature absorption spectra, e.g. 1 (blue line) in the Fig. 3.5 will follow at λ >200 nm the shape of fiber + soot absorption spectrum as shown in Fig. 3.5 by grey line.

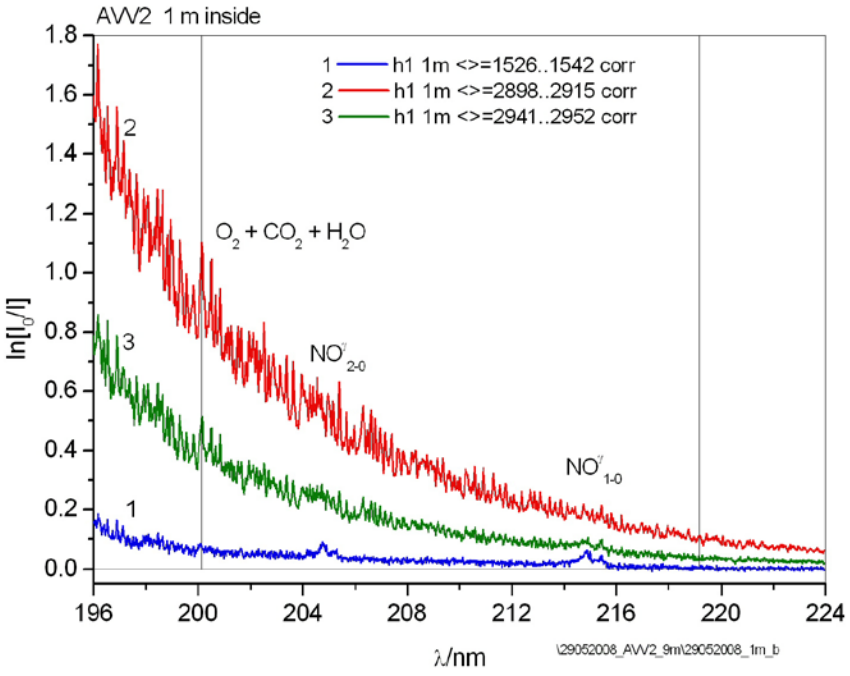

Figure 3.6: Averaged over regions 1, 2 and 3 in Fig. 3.5 corrected UV absorption spectra. Numbers correspond to various regions in Fig. 3.5. Positions of NO γ-bands are also indicated.

A gas temperature for the spectrum 1 in the Fig. 3.5 can be evaluated from the fine structure of NO γ-bands marked in the figure and it was found to be 500°C. At this temperature molecular absorption at λ >216 nm is very week and can be used for a proper match of the ($coeff_1$ • fiber + $coeff_2$ • soot) absorption spectrum to the experimental one with followed subtraction, where $coeff_1$ and $coeff_2$ are some coefficients. In the measurement sequence part of that is shown in the Fig. 3.4 there are several regions where the absorption (and consequently the temperature) is low and can be used for fiber + soot subtraction (or "correction"). Fiber + soot absorption spectrum

(grey line) was subtracted from all raw absorption spectra (1, 2 and 3) in the measurement sequence prior its followed analysis, Fig. 3.5. Corrected (i.e. after subtraction of fiber + soot spectrum) spectra are shown in Fig. 3.6. The spectra comprise of O_2, CO_2, H_2O and well-localized NO γ-bands marked in the Fig. 3.6.

As was mentioned above for the spectrum 1 in the Fig. 3.6 a gas temperature can be evaluated from the structure of NO γ(1-0) band [18]. Once the temperature is known the best set of concentrations of species under interest can be calculated by methods of linear algebra as e.g. singular value decomposition method [19]. For the spectra 2 and 3 in the Fig. 3.6 NO absorption features are hardly seen and therefore the temperature cannot directly be evaluated. Nevertheless gas temperature and gas concentrations can be obtained by selection method being used in a solution of ill-posed problems [20].

The problem of finding a best set of concentrations and temperature is directly related to solving of the inverse problem for the equation

$$Az = u_\delta, \qquad (2)$$

where *A* is a matrix of cross sections for species of interest, u_δ is an experimental (with level of error δ) absorption spectrum vector and *z* is a vector of concentrations. As well-known the straightforward way to solve the Eq. (2) as $z = A^{-1}u_\delta$ can give meaningless solutions and this is the case for our experimental data measured with a certain level of the error. Moreover CO_2, H_2O and O_2 absorption spectra all have around the same slopes with temperature that is caused a further complication (below). The way to avoid the difficulties with finding of the solution z in case of inexact right-hand part u_δ is the concept of a quasisolution of the Eq. (2) and is described in details in [20]. A quasisolution of the Eq. (2) is defined as a vector $\tilde{z}_\delta$ minimizing for a given u_δ functional difference between Az and u_δ. It is possible to exhibit sufficient conditions for $\tilde{z}$ to be unique, to depend continuously on the right hand member u_δ and finely to develop a general approach to approximate determination of quasisolutions of the Eq. (2) [20]. In practice the selection method works as followed. Among possible solutions $z_n, n = 1,..$ defined on some space possible values of the vector z we chose an element $\tilde{z}_n^\delta$ that gives the difference between $A\tilde{z}_n^\delta$ and u_δ not more than δ. This $\tilde{z}_n^\delta$ vector will be the best closed to the exact solution of the Eq. (2). Once sets of solutions $\tilde{z}_n^\delta$ at various times are obtained further data analysis can be performed by standard mathematical tools (e.g. statistics).

Analysis of the experimental spectra is more convenient to perform in logarithmic scale because on this scale absorption spectra of CO_2 and H_2O are alike straight lines relative to the wavelength, Eq. 1. The same as well holds true for overall O_2 spectrum because Boltzmann distribution over rotational levels as one can see in the Fig. 3.7 (lower panel, navy line) where the absorption spectrum 2 in the Fig. 3.6 is analyzed. The slope of the spectra depends on the temperature, whereas Y-shift is given by a concentration of

species of interest. As it can be seen from the Fig. 3.7 for the best fit spectrum (red) to the experimental one (blue) the followed features are observed: 1) underling continuum of CO_2+H_2O (black) follows with around the same slope the experimental spectrum (upper panel, blue); 2) O_2 spectrum (navy) is only add-on feature on the top of the sum of CO_2+H_2O (black) and 3) H_2O spectrum is mainly contribute to the sum of continua at λ < 206 nm and CO_2, respectively, at 218 nm < λ.

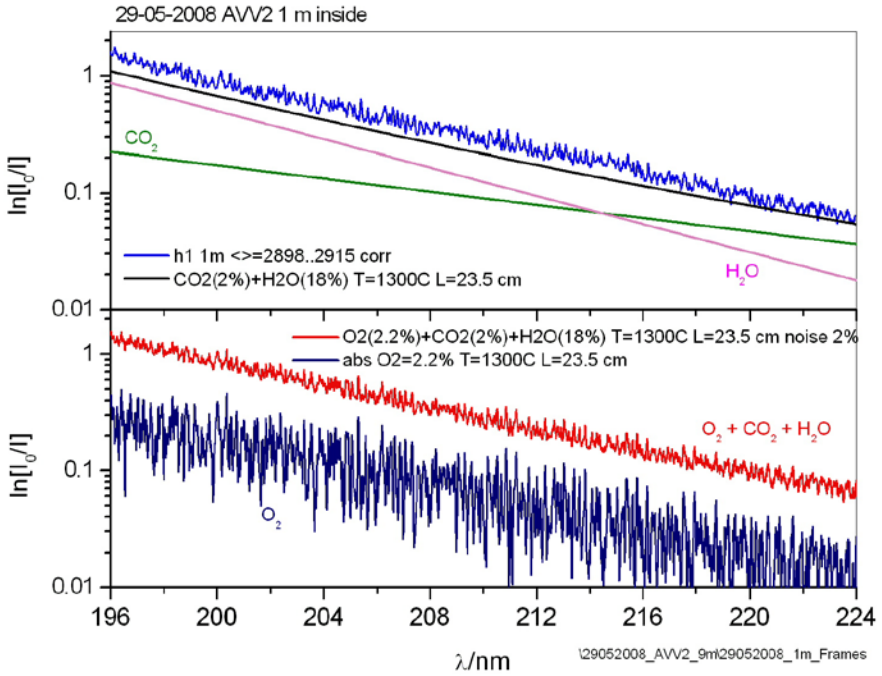

Figure 3.7: An example of experimental data analysis. Top panel: absorption spectrum 2 in the Fig. 3.6 (blue). Best fit calculated CO_2(2%) (olive), H_2O(18%) (magenta) absorption spectra and their sum (black). Low panel: best fit calculated total (red) and O_2(2.2%) (navy) absorption spectra. Best fit temperature T=1300°C.

Although a continuum CO_2+H_2O can be described by various $(z_n, a_{nj}), n = T_1, T_2, ..; j = CO_2, H_2O$ sets even at around pre-estimated (averaged) z_n values, a "best" selection of temperature (in the sense of δ) can be made on a base of ratios between minima and maxima in the fine structure of O_2 S-R absorption spectrum that should fit the experimental spectrum: lower temperatures cause less ratios even at higher z_n values. Use of the selection method for the spectrum 2 in Fig. 3.6 gives best fit concentrations of CO_2=(2 ± 0.2)%, H_2O=(18 ± 1)% and O_2=(2.2 ± 0.2)% and gas temperature of (1300 ± 80)°C.

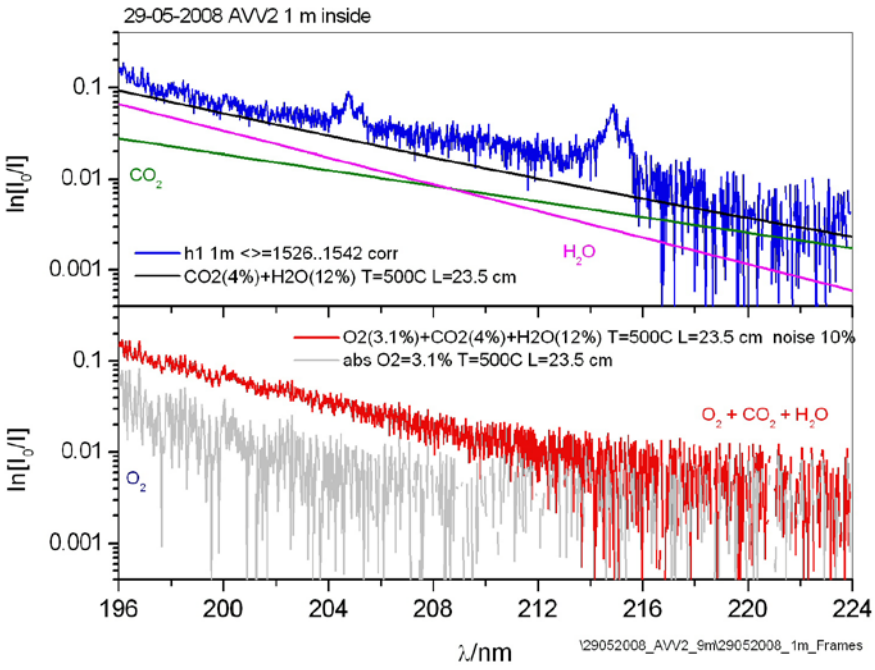

Figure 3.8: An example of experimental data analysis. Top panel: absorption spectrum 1 in the Fig. 3.6 (blue). Best fit calculated CO_2(4%) (olive), H_2O(12%) (magenta) absorption spectra and their sum (black). Low panel: best fit calculated total (red) and O_2(3.1%) (grey) absorption spectra. Best fit temperature T=500^{o}C.

Another example of data analysis is shown in Fig. 3.8 for the spectrum 1 in the Fig. 3.6. The absorption spectrum is week due to low temperature. The selection method gives best fit values concentrations for CO_2=(4 ± 1)%, H_2O=(12 ± 0.5)% and O_2=(3.1 ± 0.2)% and gas temperature of (500 ± 50)^{o}C. Since NO absorption features are more pronounced over week CO_2+H_2O absorption continuum gas temperature can be evaluated in simpler manner: from NO band shape [18]. In the analysis of spectra 1 and 2 we did not consider absorption by NO because it is well localized and gives a contribution into total absorption in the narrow spectral ranges.

The quality of the fit for spectra 2 and 1 in the Fig. 3.6 is shown in Fig. 3.9 and 3.10, respectively.

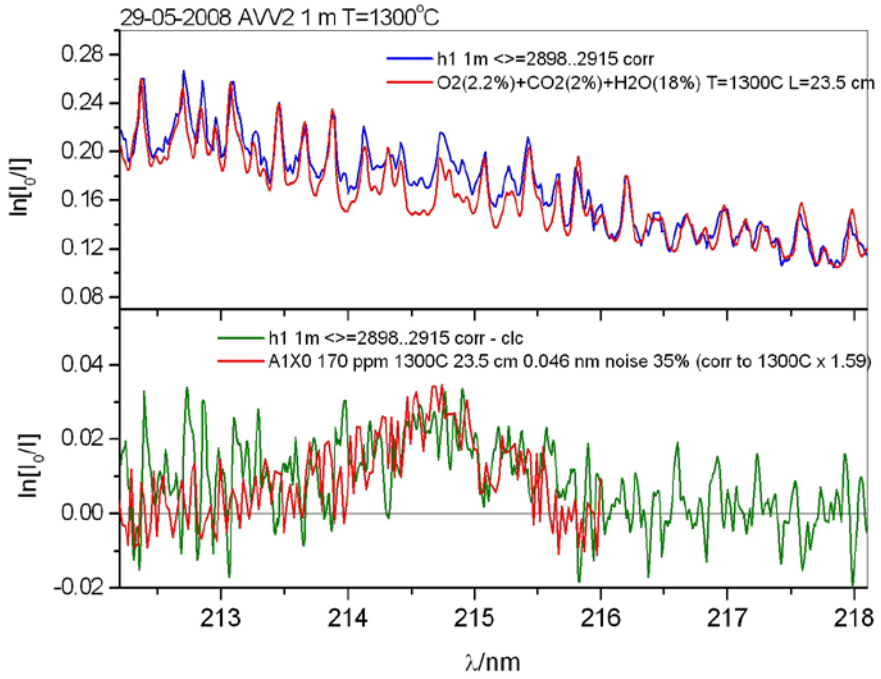

Figure 3.9: NO absorption at T=1300°C. Top panel: a part of the spectrum 2 in Fig. 3.6 (blue) and its best fit by O_2(2.2%)+CO_2(2%)+H_2O(18%) spectrum in Fig. 3.7 (red) at T=1300°C. Lower panel: residual spectrum between blue and red spectra in the top panel (olive) and calculated $NO^{\gamma}_{1\text{-}0}$ absorption band at T=1300°C and NO=170 ppm (red). Noise level 35%, $\Delta\lambda$=0.046 nm.

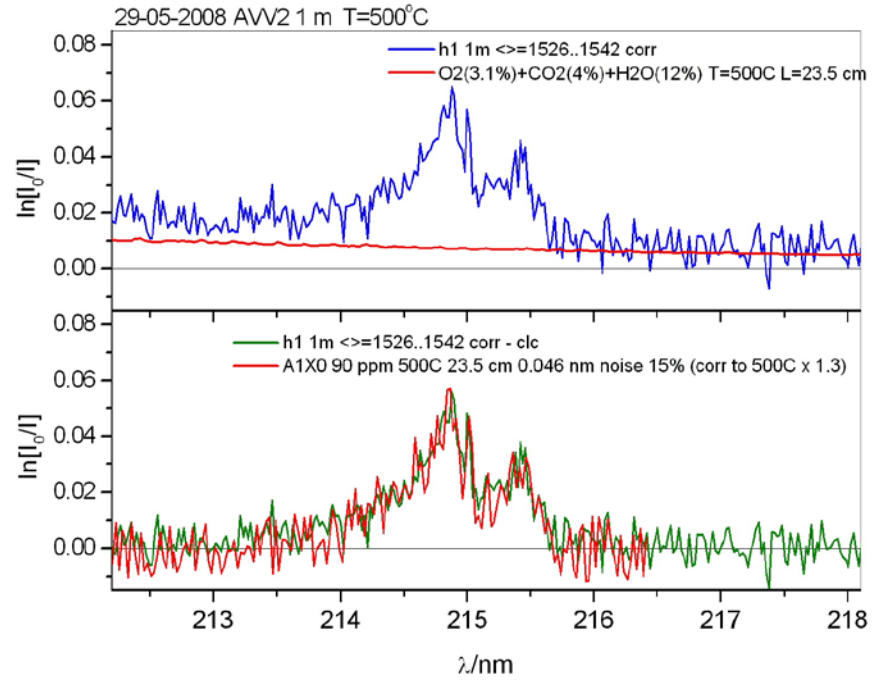

Figure 3.10: NO absorption at T=500°C. Top panel: a part of the spectrum 1 in Fig. 3.6 (blue) and its best fit by O_2(3.1%)+CO_2(4%)+H_2O(12%) spectrum in Fig. 3.8 (red) at T=500°C. Lower panel: residual spectrum between blue and red spectra in the top panel (olive) and calculated $NO^{\gamma}_{1\text{-}0}$ absorption band at T=500°C and NO=90 ppm (red). Noise level 15%, $\Delta\lambda$=0.046 nm.

The best fit O_2(2.2%)+CO_2(2%)+H_2O(18%) spectrum, Fig. 3.9 (upper panel, red) was subtracted from the experimental absorption spectrum (blue). The residual (noisy) spectrum is shown in the lower panel (olive) together with calculated NO γ(1-0) band at 1300^{o}C. The white noise was added to the calculated band shape in order match the experimental one. One can see that the experimental spectrum is described well although high noise level significantly limits a possibility of more accurate estimation of the gas temperature from the band shape. Integral over NO γ(1-0) band (without noise added) gives NO concentration of 170 ppm.

The NO γ(1-0) band region for the spectrum 1 in the Fig. 3.6 and its best fit are shown in the Fig. 3.10 (upper panel, blue and red lines, respectively). Calculated best fit spectrum O_2(3.1%)+CO_2(4%)+H_2O(12%) at 500^{o}C (red) gives a baseline without structure that is a little underneath noisy experimental spectrum. Subtracted spectrum (with small extra baseline correction) is shown in the lower panel (olive). Calculated NO γ(1-0) band at 500^{o}C with white noise (red) fits well the residual spectrum and gives NO concentration of 90 ppm. The selection method can be applied for any spectrum in time sequence shown in the Fig. 3.4. Summary of the spectra 1, 2 and 3 analysis in the Fig. 3.6 is collected in the Table 1 together with one more dataset at 1500^{o}C taken for a spectrum in the same sequence, partly shown in the Fig. 3.4, at time around 26.677 s (averaged over 20 frames).

Table 1: Summary of some selected fast (10-20 ms) UV absorption measurements at AVV2. Numbers in parentheses show the spectrum number in the Fig. 3.6

	500^{o}C (1)	900^{o}C (3)	1300^{o}C (2)	1500^{o}C (n/a)
O_2	3.1 %	2.4 %	2.2 %	1.3 %
CO_2	4 %	3.7 %	2 %	4 %
H_2O	12 %	15.4 %	18 %	14 %
NO	90 ppm	100 ppm	170 ppm	250 ppm

Variation of the absorption signal at 200.142 nm in the Fig 3.4 (blue) follows temperature variations with time. In general the absorption spectrum corresponding to the interval 1 in Fig. 3.4 shows the minimum gas temperature in this measurement sequence whereas data in the last column of the Table 1 relates the spectrum that gives the maximum absorption signal at 200.142 nm. Gas temperature evaluated from the best fit calculations as a function of the absorption signal at 200.142 nm in the experimental spectrum is shown in Fig. 3.11 (blue balls). Points in the Fig. 3.11 are well fitted by a straight line with offset 465^{o}C that is close to a temperature threshold when gas temperature can be evaluated from the UV absorption spectra of gases. The fit can be used for a quick estimation of the gas temperature at any point in the Fig. 3.4. Software for an “automatic” analysis of the complex UV absorption spectra is under development.

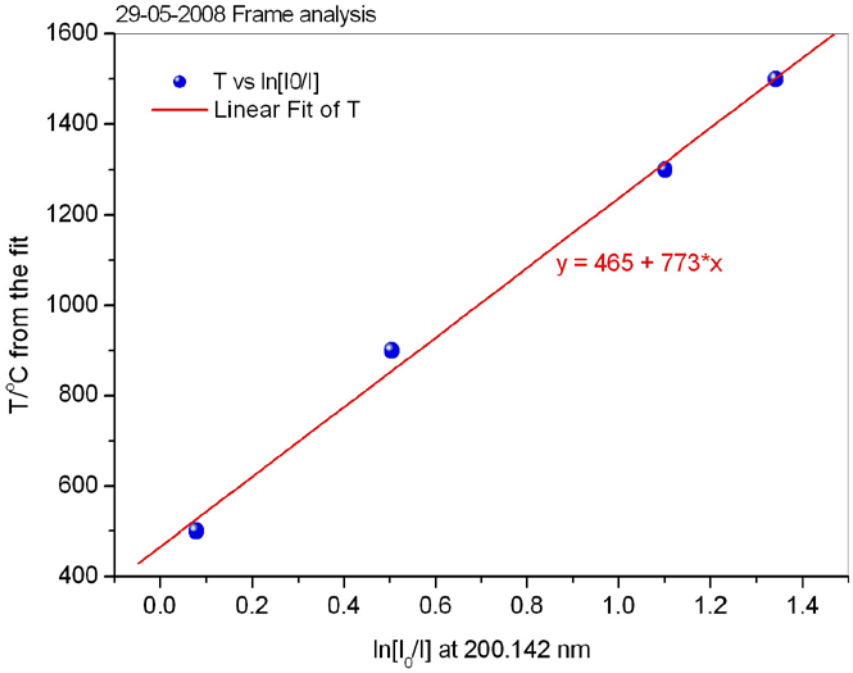

Figure 3.11: Variation of the calculated best fit gas temperature with experimental absorption signal at 200.142 nm. At absorption signal "0" the offset in the fit line 465°C that is close to the high-temperature gas detection limit for current experimental set up and gas composition for particular combustion process.

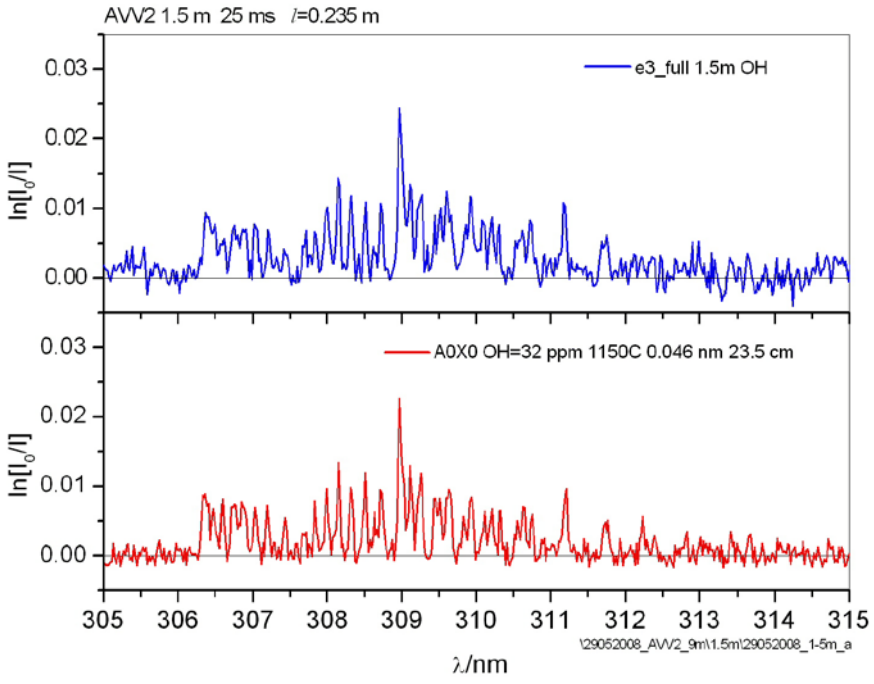

Figure 3.12: OH absorption at T=1150°C. Top panel: OH absorption spectrum measured at 1.5 m insertion (blue). Acquisition time 25 ms. Low panel: Calculated OH (A_0-X_0) absorption band at T=1150°C and OH=32 ppm (red). Noise level 8%, $\Delta\lambda$=0.046 nm.

As one can see there are rapid variations in the absorption spectra due to temperature and gas composition attributed to AVV2 lower load operation. Although measurements were focused into the fast absorption ones in 196-250 nm we also made overall measurements in broader spectral range up to 340 nm. At some probe insertions once upon the time week OH absorption at 308 nm was observed. An example is shown in the Fig. 3.12 (upper panel, blue) at 1.5 m probe insertion with acquisition time of 25 ms. Best fit of the experimental spectrum gives gas temperature 1150^{o}C and OH concentration 32 ppm, Fig. 3.12 (lower panel, red). The OH radical is produced in flames and has a short lifetime. Appearance of OH in the place where measurements have been performed (close to superheater) does evidence about fast moving flame bubbles popping upwards. We did not make simultaneous measurements in 194-224 nm and 308 nm. Therefore some points in the measurement sequence in particular at high absorption levels (> 1, Fig. 3.4) may correspond to in flame measurements.

Low load operation can cause some not foreseen features on a short time (tens of ms or s) and/or local spatial (tens of cm) scales, like observed flame bubbles at superheater level, although on a macro scale all these “splashes” are not simply observed due to low time resolution and/or gross measurements. However measurements of these transient phenomena are of interest because they influence onto macro performance of the combustion system. Thus, for example, measurements of OH radicals (by UV) is important because NO formation and fast CO (by FTIR) measurements are essential in understanding corrosion issues at low (averaged) CO values obtained by standard techniques.

A residence time of the hot gas in the UV optical head gas absorption part, Fig. 3.1, is around 3-5 ms. On this time scale cooling of the gas by “cold” body of the optical head is taking place only in very thin boundary layer and dos not effect into measurements in the central (“bulk”) gas absorption part. Therefore gas temperature calculated from the Fig. 3.4 and 3.12 or from spectra shown in the Fig. 13 is a *true* temperature of the hot gas.

3.3.4 Gas extraction at 1 m probe insertion

In order to verify UV absorption technique and data analysis approach gas extraction measurements were also performed. The extraction system [21] includes a water-cooled probe for extraction of particles and gases, a particle filter, two 50 cm long gas cells for simultaneous UV/IR-absorption measurements, a sophisticated paramagnetic oxygen analyzer, calibrated mass-flow controllers and a pump. The data acquisition system allows continuously record the main sampling parameters such as extraction gas flow, gas temperature, pressure in the UV/IR gas cells and the oxygen concentration. The temperature in the extraction line from the probe tip to the gas cells is kept constant at 150^{o}C by electronically controlled heaters. A Bomem MB155 FTIR spectrometer ($\Delta\nu$ = 2 cm^{-1}) with the built-in IR light source and external DTGS detector were used for the IR-absorption measurements. A D_2 UV lamp is utilized as a light source and UV-absorption spectra were recorded with the same UV spectrometer as described in the Ch. 2.3.

Response time of the extraction system depends on the probe and extraction line lengths and for these trial measurements was around 10 s. Response time of the oxygen analyzer alone is 3.5 s. The water-cooled probe for gas extraction was fixed onto the 9-m probe by

metal fasteners. The inlet hole of the gas extraction probe was placed in the middle part of the optical head. Gas extraction measurements have been performed in parallel with fast UV absorption ones. The 9-m probe was inserted by 1 m inside of the boiler. Because the UV spectrometer was used for the fast UV absorption measurements with 9-m probe, only O_2 (by oxygen analyzer) and CO_2, H_2O (by FTIR spectrometer) measurements have been made. Variations in oxygen concentration measured by paramagnetic oxygen analyzer during fast UV absorption measurements were in between 4.8 to 5.5 % that is a little more than for those obtained from the UV absorption measurements, Table 1. However as it can be seen from the Fig. 3.4 and Table 1 during measurements temperature and oxygen concentration are rapidly changed from 500^{o}C to 1500^{o}C and from 3.1 to 1.3 %, respectively. For some points in the Fig. 3.4 oxygen concentration might also be higher or lower of those in the Table 1. The same is also valid for CO_2 concentration time behavior because in general CO_2 follows in opposite to O_2 variations. Water content, however, is relatively stable in time as one can expect, Table 1. Although the maximum of the NO absorption band decreases (at the same NO concentration) if the temperature is raised, it is clearly seen increase of the nitrogen oxide concentration with the temperature that is well-known effect in combustion.

In the Table 2 concentrations of O_2, CO_2 and H_2O obtained with gas extraction system are collected together with data from AVV2 log-file for around the same sampling time. It should be noted that gas extraction data show a *local* gas composition *in the boiler* whereas data from AVV2 log file represent *averaged over net flue gas flow* measurements in the hot gas duct in the vicinity of AVV2 economizer. One can see there is a reasonable agreement between both data sets.

Further verification of the UV absorption technique could be done by e.g. *in situ* FTIR gas temperature and composition measurements [1].

Table 2: Gas composition data averaged over time (3-10 s) obtained from extraction measurements and AVV2 log file in the same time when fast UV absorption measurements were made.

Gas Extraction Data	AVV2 log file Data
O_2 = 5.2%	O_2 = 0-9% (unstable)
CO_2 = 7.3%	CO_2 = 6.3%
H_2O = 12.4%	NO = 85.7 ppm

4 Time-resolved fast NO UV absorption measurements on a large ship engine

A concept of fast time/spectral-resolved measurements described in the Ch. 3 has been used in measurements on a large ship engine at MAN Diesel facilities in Copenhagen. Measurement campaign was performed under EU founded HERCULES-B project about high efficiency engines with ultra-low emissions for ships.

Experimental layout is shown in Fig's. 4.1-3. Measurements were performed across exhaust gas flow in specially designed and made exhaust pipe with three optical access ports. The exhaust pipe was mounted on the top of the cylinder after cylinder's exhaust valve. Optical absorption pathlengths were calculated as 15.1, 22.5 and 15.1 cm for top, middle and low ports, respectively. A stand-alone D_2-lamp was used as an UV light source. The spectra were recorded with the spectrometer described in the Ch. 2.2. The spectrometer and lamp were coupled to the measurement locations by two UV-advanced optical fibers. Effective acquisition time for each absorption spectrum was 5.4 ms.

Pressure in the exhaust pipe was measured by two pressure sensors placed from top and bottom sides in the pipe. Some measurements were also supplied by simultaneous gas temperature measurements with thermocouples (TC's) mounted together with pressure sensors. However TC's gave only averaged values and were quickly broken during engine operation. External synchronization trigger signal has been used for acquisition of UV absorption spectra and pressure at various values of piston crank angle (or at various time steps).

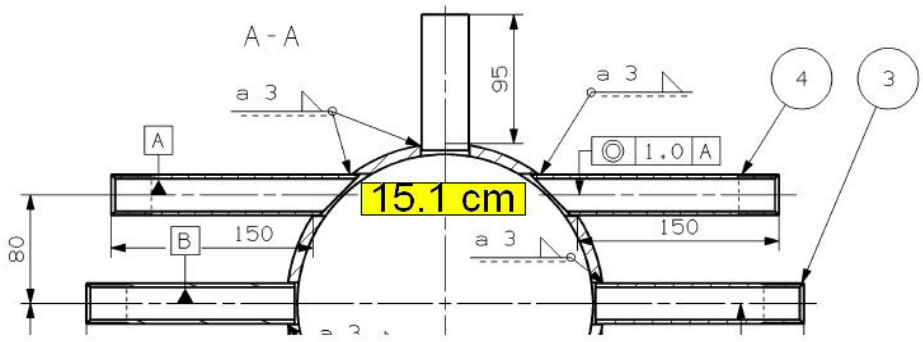

Figure 4.1: A part of exhaust pipe with marked area in yellow used for UV absorption measurements at top location, *L*=15.1 cm.

Typical UV absorption spectra for some selected frames (or time steps) during one cycle (0.54 s) are shown in Fig. 4.4 for top measurement location. The spectra consist from several strong NO absorption bands and a weak nearly flat continuum (scattered light and soot absorption). The very first and last panels (frames #515 and #550, respectively) show residual NO absorption in the exhaust pipe whereas two middle panels (frames #525 and #535) show variations in NO concentration after opening the exhaust valve. Appearance of 0-1 NO band at 237 nm (frame #525) indicates that the temperature of the gas is more than 300^{o}C.

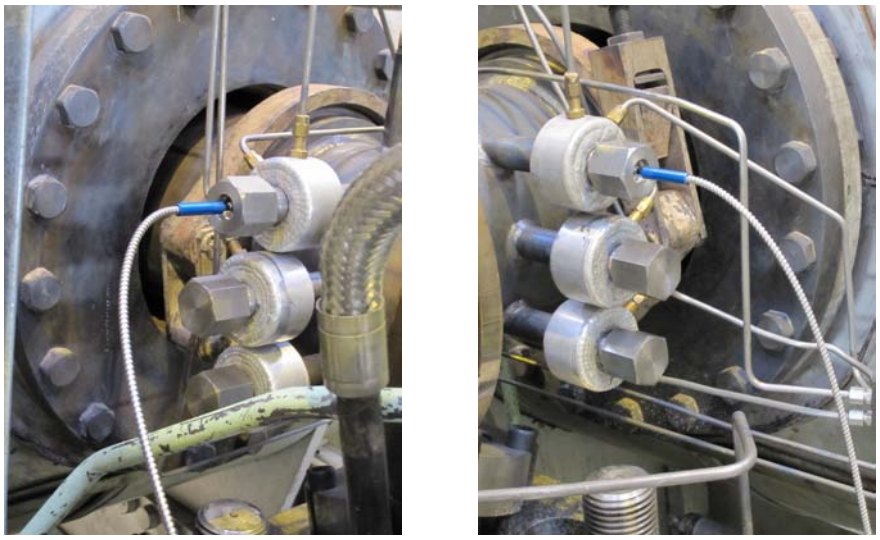

Figure 4.2: Left: UV optical fiber connected to the left port (top location) and to the spectrometer. Right: UV optical fiber connected to the right port (top location) and to the UV-lamp.

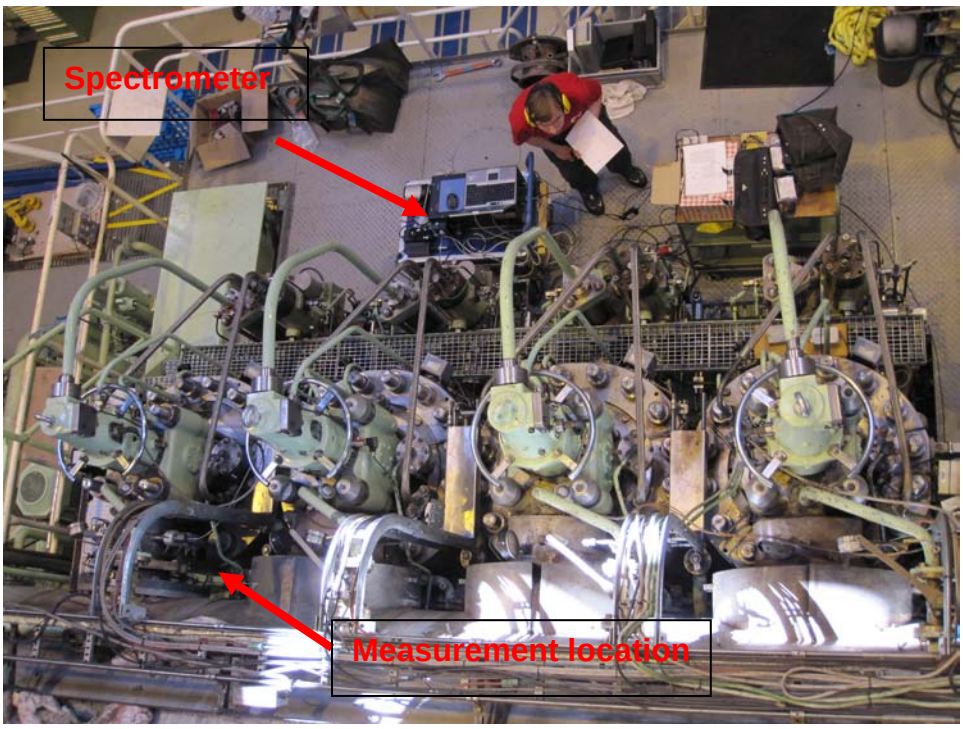

Figure 4.3: Optical layout and measurement location, top view. Measurements were performed on one out of four cylinders.

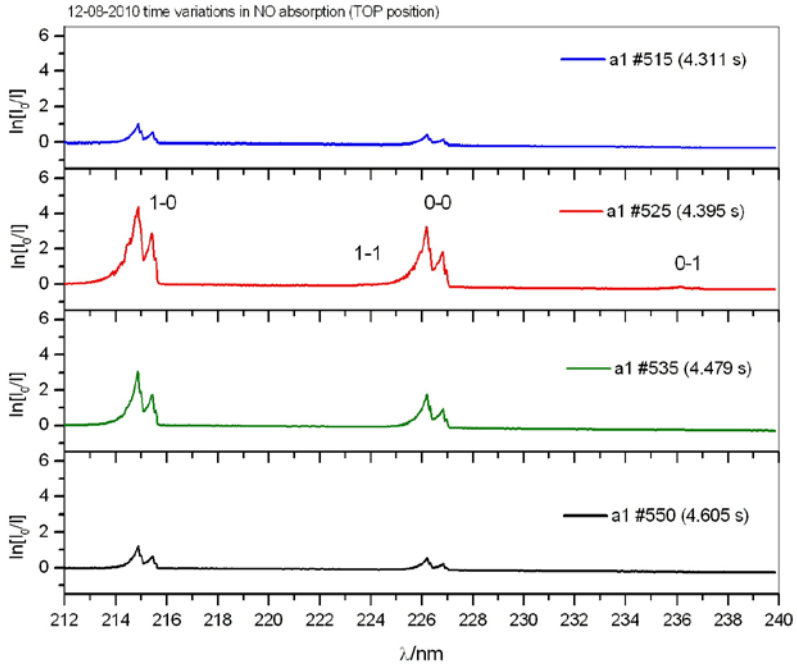

Figure 4.4: Typical time variations in UV absorption spectra during one cylinder cycle for some selected frames: #515, 525, 535 and 550 (top location). Each spectrum corresponds to 5.4 ms effective acquisition time. NO absorption bands are marked.

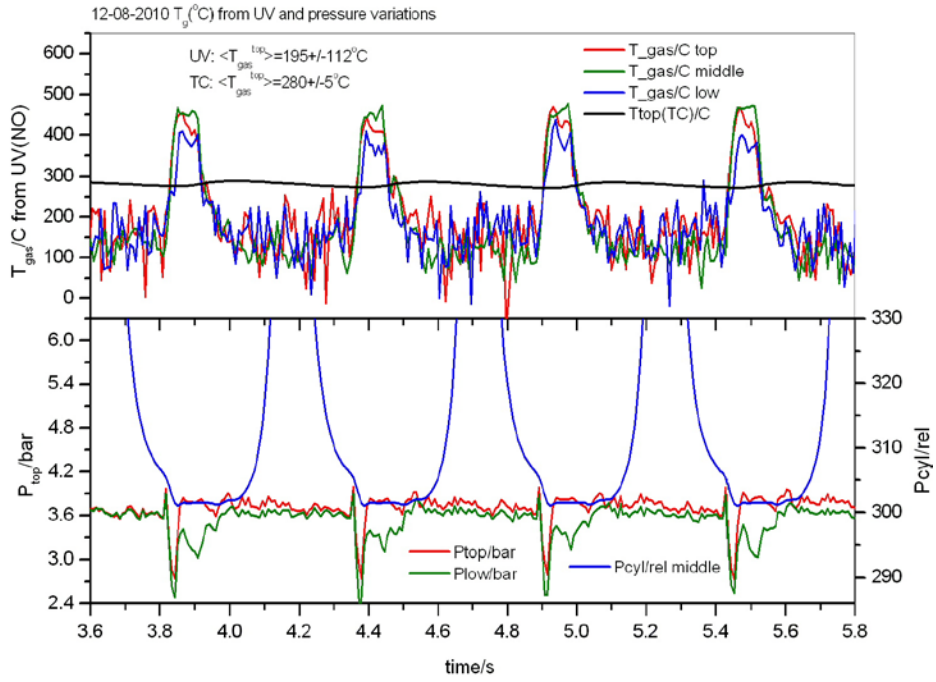

Figure 4.5: Upper: gas temperature variations at three locations (top (red), middle (olive), low (blue)) calculated from NO UV absorption band at 226 nm and from TC measurements at top location (black). Lower: pressure variations in the cylinder (blue) and at top (red) and low (olive) locations in the exhaust pipe.

Gas temperature was calculated from the fine structure on the NO absorption bands measured at $\Delta\lambda$=0.046 nm spectral resolution. This structure depends mainly on gas temperature and to less extend pressure (pressure broadening). Accuracy of the gas temperature calculations is about 50^{o}C for good "signal-to-noise" measured spectra, e.g. in Fig. 4.4. Calculated gas temperatures at three measurement locations in the exhaust pipe are shown in Fig. 4.5 (upper panel) for four piston cycles. In the same figure pressure variations in the exhaust pipe and in the cylinder are also shown (lower panel). Sharp deeps in pressure correspond to the moment when the exhaust valve is opened and may be attributed to Bernoulli's effect. As can be seen the gas temperature at low location is lower compare to that at top and middle locations. TC measurements at top location show "averaged" gas temperature because the TC shows it own temperature effected by mass flow propagation. Simple averaging gives 195^{o}C (±112^{o}C) and 280^{o}C (±5^{o}C) for T_g calculated from UV and TC measurements, respectively.

Knowing temperature and pressure NO concentration in the exhaust pipe can be calculated. Because strong NO absorption, deviations from Lambert-Beer law have to be taken into account. Calculated NO concentrations for the same time scale as in the Fig. 4.5 are shown in Fig. 4.6 (upper panel). There are small variations in NO concentration from cycle-to-cycle at measurement locations. In the same figure pressure variations as in the Fig. 4.5 are also shown for the reference. When the valve is opened the hot gas from the cylinder is quickly cooling down due to it expansion, Fig. 4.5.

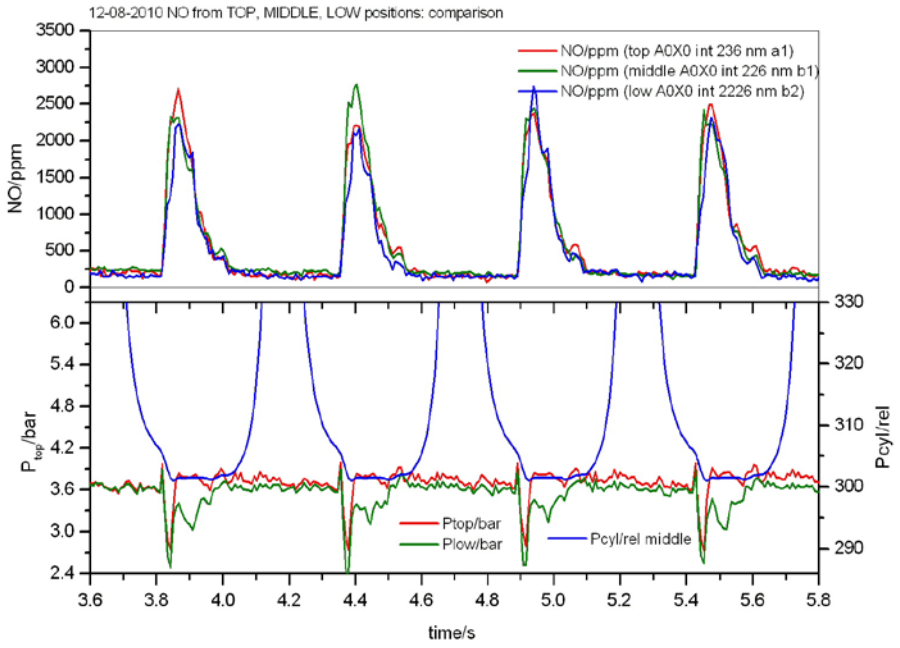

Figure 4.6: Upper: NO concentration variations at three locations (top (red), middle (olive), low (blue)) calculated from NO UV absorption band at 226 nm. Lower: pressure variations in the cylinder (blue) and at top (red) and low (olive) locations.

NO concentration reaches peak level about 2900 ppm in about 50 ms after the exhaust valve is opened, Fig's. 4.7-9.

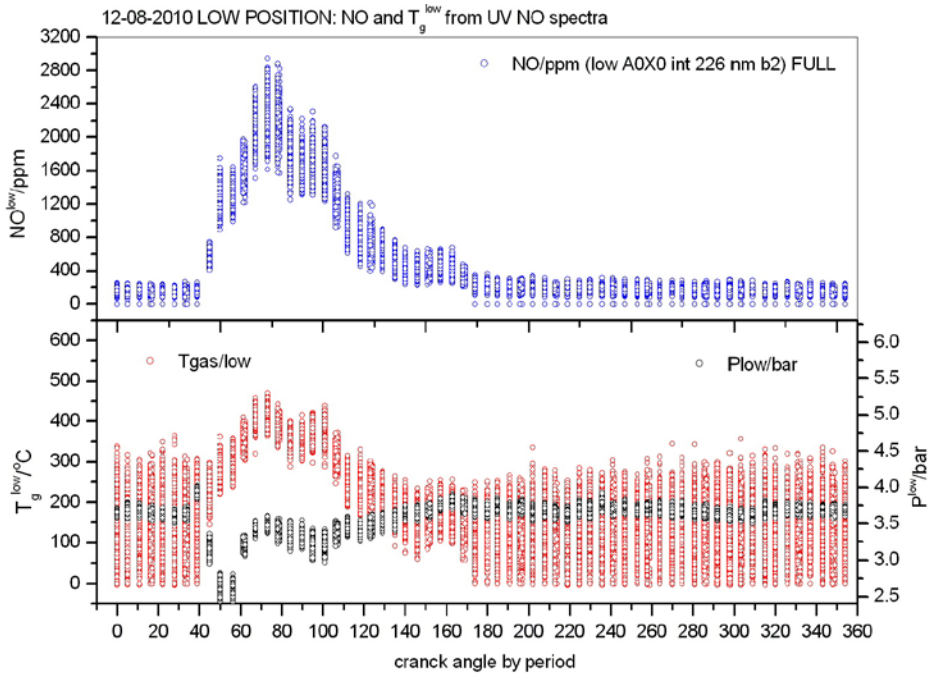

Figure 4.7: Upper: NO concentration variations at low location at various crank angles. Lower: gas temperature (red) and pressure (black) variations at low location with crank angle over 625 engine cycles.

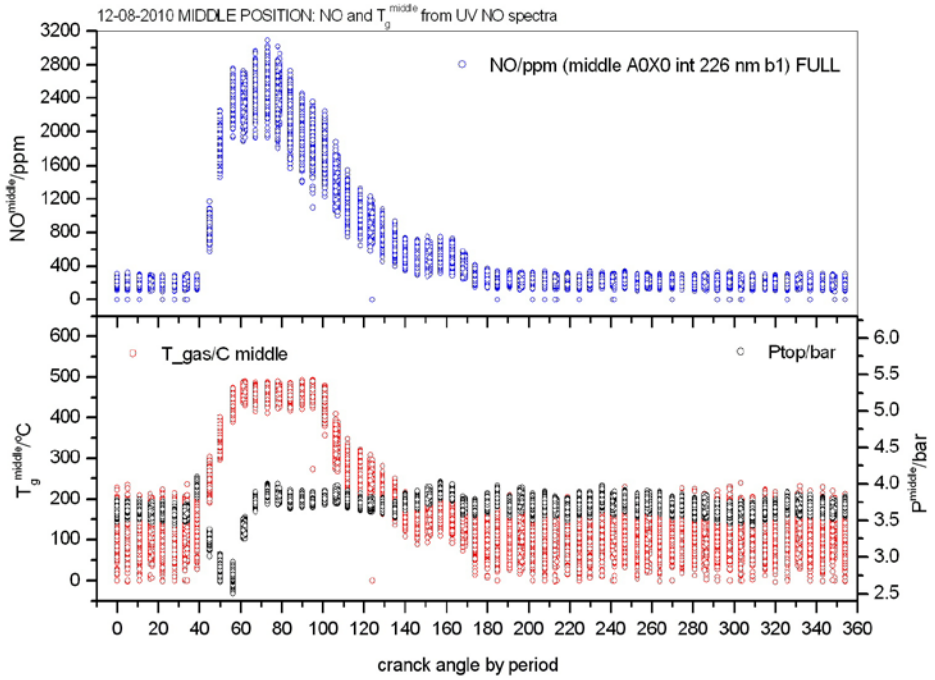

Figure 4.8: Upper: NO concentration variations at middle location at various crank angles. Lower: gas temperature (red) and pressure (black) variations at middle location with crank angle over 625 engine cycles.

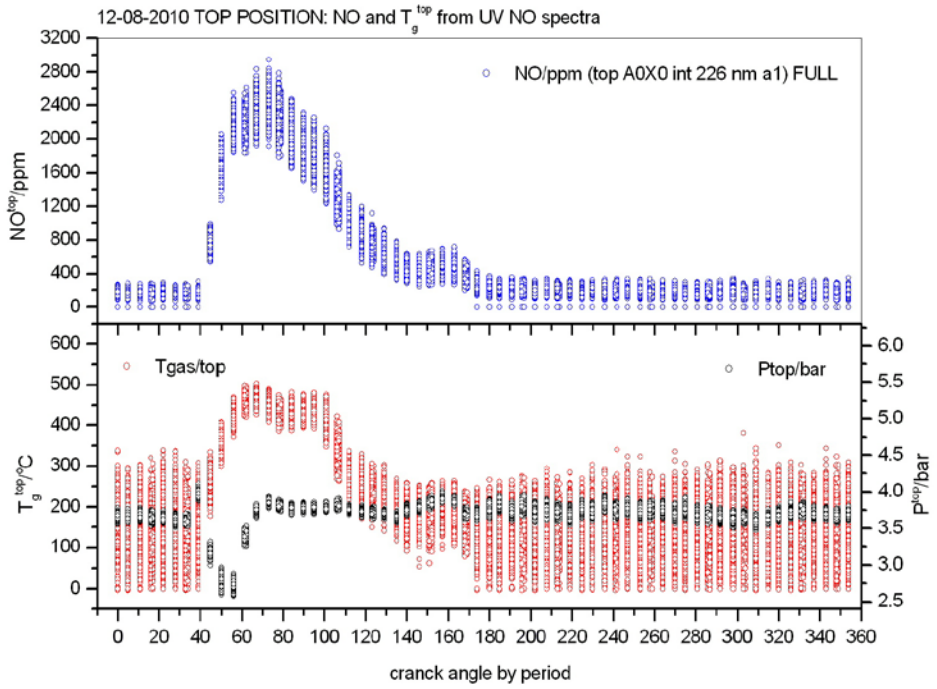

Figure 4.9: Upper: NO concentration variations at top location at various crank angles. Lower: gas temperature (red) and pressure (black) variations at low location with crank angle over 625 engine cycles.

As one can see (statistically) NO concentrations and gas temperatures are about the same for the upper and middle locations. However at low location NO concentration and gas temperature is less to about 200 ppm and 25°C, respectively. Because of the bend of the exhaust pipe difference in the gas temperatures and NO concentrations may be explained by flow patterns of the hot gas in the pipe. The NO level is somewhat may be expected from diesel engines [22].

In the same measurement campaign newly developed fast IR optical system was also used [21]. The system is designed for measurement of gas temperature and gas composition (e.g. CO, CO_2, H_2O) with 1 ms time resolution and has been developed in Energinet.dk project No. 2008-1-0079. The system includes a fast IR camera coupled to an IR spectrometer, a set of IR fibers and IR optics. The system has been successfully used in flame measurements on a power plant [21] (Energinet.dk project No. 2007-7333).

Gas temperature was calculated from CO_2 band at 2340 cm^{-1} by emission/absorption method. Comparison between UV (NO) and IR (CO_2) methods for gas temperature calculation is shown in Fig. 4.10. Gas temperature measurements by TC at the top position are also shown. It should be noted that UV and IR measurements were performed at the same engine running settings but at different times. Although there is an offset in T_g(IR) at top and low locations between subsequent exhaust valve openings agreement between T_g(UV) and T_g(IR) is quite well. UV and IR measurements both give lower gas temperature at low measurement location compare to that at middle and top locations when the valve is opened. Therefore only one UV sensor can be used for measurements of NO concentration.

Once the valve is opened fast expending and cooling down exhaust gas transfers the heat to TC which shows rise of its own temperature, Fig. 4.10 (black line).

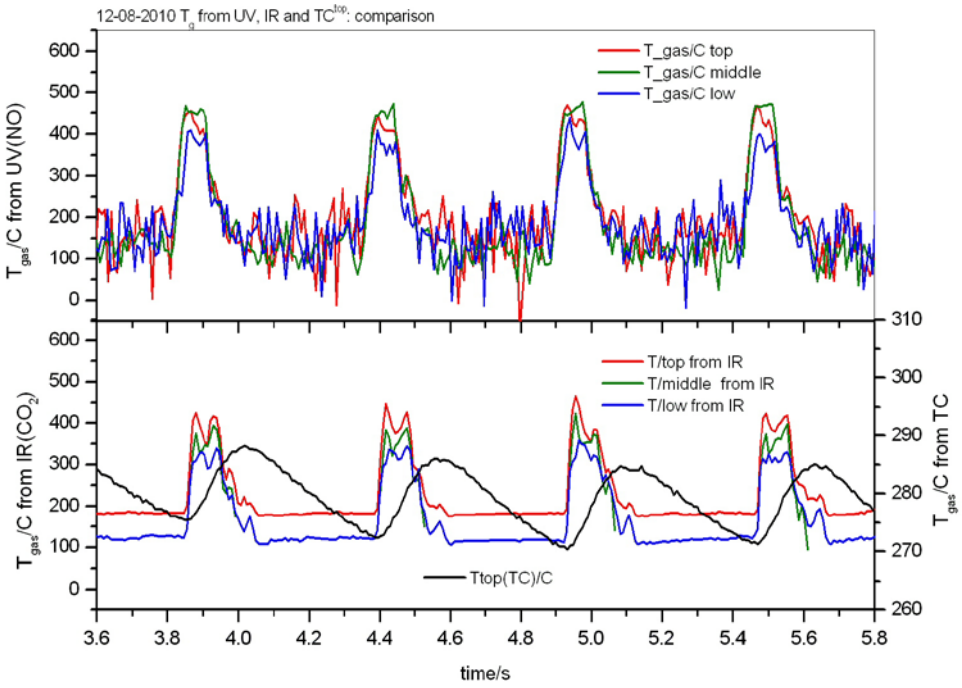

Figure 4.10: Upper: gas temperature variations at three locations (top (red), middle (olive), low (blue)) calculated from NO UV absorption band at 226 nm. Lower: gas temperature variations at three locations (top (red), middle (olive), low (blue)) calculated from CO_2 IR absorption band at 2340 cm^{-1}. Gas temperature from TC measurements is indicated by black line.

Measurements performed in the exhaust pipe of the cylinder shown a possibility of fast time-resolved NO UV absorption measurements. Gas temperatures calculated from UV (NO-based) and IR (CO_2-based) time-resolved optical absorption spectra are in quite well agreement with each others. Gas temperature and NO concentration vary quickly upon exhaust valve opening. Therefore NO UV absorption spectra can be used for both gas temperature and NO concentration on-line measurements on large ship engines. Because simplicity of the UV absorption spectra in the region of NO absorption bands, Fig. 4.4, there is a possibility for hard-, soft-ware development towards an “automatic” robust on-line NO/T gas analyzer.

5 Conclusions

The main conclusions made during the project are:

- Combined IR and UV spectroscopy set up on high temperature gas cells is developed;
- System combing UV fiber optic head and 9-m water cooled probe has been developed and tested. The optic head can also be used for IR *in situ* measurements;
- The system has successfully tested on a full scale boiler. Software for an "automatic" analysis of the complex UV absorption spectra is under development.;
- Developed concept has been applied for fast time-resolved NO and gas temperature measurements on a large ship engine. There is a possibility for future hard-, soft-ware development towards an "automatic" robust on-line NO/T gas analyzer. ;

The concepts and spectroscopic gas data measured in the project will be useful in the future energy projects. Nevertheless, future work is needed to extend, validate and improve performance of such measurements in research and full-scale energy systems.

6 References

[1] S Clausen *Meas. Sci. Technol*. **7** (1996) pp. 888-896

[2] A Leipertz and M Wensing *J. Phys.:Conference Series* **85** (2007) p. 012001

[3] W Von Drasek, AP Melsio, S Wehe, M Allen in: A Wang (Ed.) *Sensors for Harsh Environments II, Proc. of SPIE* (2005) 5998 59980E

[4] R Obertacke, H Wintrich, F Wintrich, A Leipertz *Combust. Sci. and Tech.* **121** (1996) pp. 133-151

[5] T Fleckl, H Jäger, I Obernberger in: R Tinto (Ed.) *Proc. of the 5th Conference on Industrial Furnaces and Boilers*, Porto, Portugal, 2000

[6] DONG Energy A/S: http://www.dongenergy.com/EN/business+activities/generation/electricity+generation/Primary+power+stations/Avedore+Power+Station.htm

[7] A Fateev and S Clausen *On-line non-contact gas analysis*, Risø-R-1636(En), Risø DTU, March 2008, ISBN 978-87-550-3659-8, 24 p.

[8] S Clausen KA Nielsen and A Fateev *Ceramic high temperature gas cell operating up to 1873 K*. to be published.

[9] MPI-Mainz-UV-VIS-Spectral Atlas of Gaseous Molecules, Ed. H. Keller-Rudek, G.K. Moortgat, Max-Planck-Institut für Chemie, Atmospheric Chemistry Division, Mainz, Germany, www.atmoshere.mpg.de/enid/2295

[10] C Schulz, JB Jeffries, DF Davidson, JD Koch, J Wolfrum, RK Hanson *Proc. Combust. Inst.* **29** (2002) pp. 2735-2742

[11] SL Manatt and AL Lane *J. Quant. Spectrosc. Radiat. Transfer* **50**(3) (1993) pp. 267-276

[12] MH Palmer, DA Shaw, MF Guest *Mol. Physics* **103**(6-8) (2005) pp. 1183-1200

[13] J Vattulainen, L Wallenius, J Stenberg, R Hernberg, V Linna *App. Spect.* **51**(9) (1997) pp. 1311-1315

[14] J Mellqvist and A Rosen *J. Quant. Spectrosc. Radiat. Transfer* **56**(2) (1996) pp. 187-208

[15] D Lucas, MD Morrow, NJ Brown *Proc. Combust. Inst.* **20** (1984) pp. 1313-1320

[16] J Bak and S Clausen *Meas. Sci. Technol*. **13** (2002) pp. 150-156

[17] G Basile, A Rolando, AD'Alessio, AD'Anna, P Minutolo *Proc. Combust. Inst.* **29** (2002) pp. 2391-2397

[18] A Fateev and S Clausen *Int. J. Thermophys*, 2008, DOI 10.1007/s10765-008-0438-5

[19] CL Lawson, RJ Hanson *Solving Least Squares Problems*, Prentice-Hall, Inc., Englewood Cliffs, N.J., 1974

[20] AN Tikhonov and VY Arsenin *Solutions of Ill-posed Problems*, John Wiley, New York, 1977

[21] J Beutler, S Clausen, V Evseev, A Fateev and SL Hvid *Combustion zone investigation in fuel flexible suspension fired boilers, Experimental*, Risø-R-1751(EN), October 2010

[22] K Verbiezen, AJ Donkerbroek, RJH Klein-Douwel, AP van Vliet, PJM Frijters, XLJ Seykens, RSG Baert, WL Meerts, NJ Dam, J.J. ter Meulen *Combustion and Flame* 151 (2007) pp. 333–346

Risø DTU is the National Laboratory for Sustainable Energy. Our research focuses on development of energy technologies and systems with minimal effect on climate, and contributes to innovation, education and policy. Risø has large experimental facilities and interdisciplinary research environments, and includes the national centre for nuclear technologies.

Risø DTU
National Laboratory for Sustainable Energy
Technical University of Denmark

Frederiksborgvej 399
PO Box 49
DK-4000 Roskilde
Denmark
Phone +45 4677 4677
Fax +45 4677 5688

www.risoe.dtu.dk